Generation and reduction of bulk nanobubbles by ultrasonic irradiation

Keiji Yasuda[a*], Hodaka Matsushima[a], Yoshiyuki Asakura[b]

[a] *Department of Chemical Systems Engineering, Graduate School of Engineering, Nagoya University, Furo-cho, Chikusa-ku, Nagoya 464-8603, Japan*

[b] *Honda Electronics Co., Ltd., 20 Oyamazuka, Oiwa-cho, Toyohashi 441-3193, Japan*

Email: yasuda.keiji@material.nagoya-u.ac.jp

Abstract

To develop a compact generator of bulk nanobubbles (ultrafine bubbles), ultrasound was irradiated to ultrapure water. Effects of ultrasonic power and frequency on nanobubble concentration and diameter were investigated. Nanobubbles with a diameter of 90 - 100 nm were generated. Number concentration of nanobubbles increased with time and approached asymptotically to an equilibrium value which was about 1.5×10^9 mL^{-1}. Nanobubble concentration increased with increasing ultrasonic power and decreasing frequency. For comparison, ultrasound was also irradiated to high concentration nanobubble water prepared by pressurized dissolution method. Reduction of nanobubbles was measured and nanobubble concentration decreased to the equilibrium value. Nanobubble concentration decreased with increasing ultrasonic power and frequency.

Generation and reduction of nanobubbles by ultrasound was modeled to analyze experimental data. The generation rate coefficient of nanobubbles increased with decreasing frequency because cavitation collapse became stronger. The reduction rate constant of nanobubbles at 488 kHz and 1 MHz in high concentration nanobubble water became much higher than those in ultrapure water due to aggregation and floatation of nanobubbles. The equilibrium number concentration increased with decreasing frequency. The results calculated by our model were in good agreement with the experimental data. The nanobubble generator using ultrasound is compact, simple in operation and

produce nanobubbles in a short time. This method is contamination-free because the liquid pump is unnecessary.

Keyword

Bulk nanobubbles, Ultrasound, Frequency, Ultrapure water, Number concentration, Ultrafine bubbles

1. Introduction

Small bubbles, which have a diameter of less than 1 μm, are called nanobubbles. Nanobubbles usually exist in two forms: nanobubbles trapped on solid surface are known as surface nanobubbles and nanobubbles dispersed in bulk liquid are known as bulk nanobubbles. Alternative and equivalent term of bulk nanobubbles is ultrafine bubbles (Alheshibiri et al., 2016). Bulk nanobubbles have very long life in water because rise velocity by buoyancy is negligibly low. They are able to persist for more than two months (Ebina et al., 2013). They also have bioactivity (Liu et al., 2016) and are negatively charged on the surface in a neutral region (Oh and Kim, 2017). Water containing nanobubbles attracts great attention in many fields of cleaning (Wu et al., 2008; Ushida et al., 2012; Zhu et al., 2016), agriculture (Ebina et al., 2013; Liu et al., 2013; Minamikawa et al., 2015; Schenk et al., 2015; Liu et al., 2016), wastewater treatment (Agarwal et al., 2011; Temesgen et al., 2017), medicine (Safonov and Khitrin, 2013; Noguchi et al., 2017), surface treatment (Matsuno et al., 2014), fuel (Oh et al., 2013), and fisheries (Ebina et al., 2013). These bulk nanobubbles have no shell. The stability mechanism of nanobubbles without shell is unclear and under discussion (Yasui et al., 2016).

To generate water containing nanobubbles, several type generators using membrane, static mixer, swirl liquid flow, and pressurized dissolution have been developed. In membrane method (Kukizaki and Goto, 2006), water containing a surfactant flows into the inside of a tubular glass

membrane and pressurized gas is injected from the outside of the membrane. Nanobubbles are generated at the inside surface of the membrane and their diameter is around 400 nm. However, the addition surfactant to water is needed to generate nanobubbles. In static mixer (Mogami and Nakata, 2014) and swirl liquid flow (Tsuji, 2013) methods, gas-liquid two-phase fluid is introduced into the static mixer and the swirl flow chambers, respectively and bubbles are crushed into nanobubbles due to shear stress. In pressurized dissolution method (Maeda et al., 2014), gas-liquid two-phase fluid flows in a pipe which has expansion and contraction parts. Gas dissolves into water at the expansion part and nanobubbles are generated after passing through the contradiction part. All generators require a liquid pump which is available for gas-liquid two-phase fluid. The operation time is long because gas-liquid fluid circulates between generator and sample tank many times. Generator size is relatively large and the large amount of liquid is required. Gas is continuously supplied to liquid. It is desired to develop a generator which is compact, simple in operation and produces nanobubbles in a short time.

When ultrasound is irradiated to water, fine bubbles occur from bubble nuclei, grow to about resonance size under acoustic pressure fluctuations, and collapse (Leighton, 1994). This phenomenon is termed acoustic cavitation and applies to apparatus such as homogenizer (Miastkowska et al., 2017) and cleaner (Luján-Facundo et al., 2016). Moreover, in medical area, microbubbles, which have a diameter of 1 - 100 μm, have been used as a contrast medium in ultrasonic diagnosis (Cosgrove, 2006). Recently, nanobubbles are applied to not only ultrasonic diagnosis (Cai et al., 2015; Yang et al., 2015; Wang et al., 2017) but also therapy (Jing et al., 2016; Suzuki et al., 2016; VanOsdol et al., 2017). Though acoustic cavitation derives from fine bubbles without shell, nanobubbles used in ultrasonic diagnosis and therapy mostly have the stabilizing shell (denatured albumin, surfactants or phospholipids). Thus, ultrasound in liquid have a close relation to fine bubbles. There is possibility that ultrasound irradiation to water generates nanobubbles during the growth process from bubble nuclei to cavitation bubbles.

In this study, ultrasound was irradiated to ultrapure water. The change of number concentration

and diameter of nanobubbles with irradiation time was investigated in various ultrasonic frequency and power. Moreover, ultrasound was irradiated to water containing high-concentration nanobubbles. A simple model is proposed to explain generation and reduction of nanobubbles by ultrasonic irradiation.

2. Experimental methods

Fig. 1 shows outline of experimental apparatus. Driving ultrasonic frequencies were 22, 43, 129, 488 kHz and 1 MHz. A Langevin transducer with multiple frequencies (HEC45242M, Honda Electronics) was used at 22, 43, and 129 kHz and its diameter was 45 mm. Disc type transducers (Honda Electronics) with 50 mm in diameter were used at 488 kHz and 1 MHz. An inside diameter of vessel was 56 mm. The vessel and vibration plates with a transducer were made from stainless steel. The transducer was fixed at the bottom of the reactor, and ultrasound was irradiated on to the sample in the vessel. The vessel had double layer structure and a circulating water bath was connected to the annular section of the vessel to maintain the sample temperature at 298 ± 1 K.

Transducers were driven by a power amplifier (1040L, E&I) which amplified a continuous sinusoidal wave produced by a signal generator (1942, NF). Except for 488 kHz, impedance matching circuits (Honda Electronics) were connected between the power amplifier and the transducer to match the impedance of transducers. An effective electric power applied to transducers was calculated from a voltage at both ends of the transducers and a current measured by an oscilloscope (TDS3014B, Tektronix) and a current probe (TCP202, Tektronix), respectively. To keep the electric power applied to the transducer constant, the effective electric power was transferred to a personal computer via a general-purpose interface bus (GPIB) and the amplitude of the signal was controlled using a computer program (Honda Electronics). The ultrasonic power that is the energy applied to the sample per unit time was obtained by calorimetry.

Ultrapure water and water containing high concentration of bulk nanobubbles were used as

samples. Ultrapure water was produced using systems equipped with both Elix-UV20 and Milli-Q Advantage for laboratory use (Millipore). Initial dissolve oxygen in ultrapure water was 8.0 - 8.3 mg/L. Water containing high concentration of nanobubbles was prepared from ultrapure water by pressurized dissolution method (ultrafineGaLF, IDEC). Hereafter, water containing high concentration of nanobubbles is abbreviated to nanobubble water. Gas in nanobubbles was air. After preparation of nanobubble water, the sample were left to stand for 2 days to remove microbubbles and obtain a stable dissolved oxygen in water. Initial dissolve oxygen in nanobubble water was 8.0 - 9.0 mg/L. Sample volume was 100 mL. The bubble diameter distribution in the range from 30 nm to 1000 nm was measured by nanoparticle tracking analysis method (NanoSight, Malvern). Number concentration of nanobubbles which is defined as the total bubble number of 30 - 1000 nm in diameter per one milliliter, and mode diameter of nanobubbles were obtained. The sample were left to stand for 5 minutes after ultrasonic irradiation to remove large microbubbles, and measurement was performed. At the measurement of nanobubbles, we chose the place without microbubbles because microbubbles disturb measurement. Measurement was conducted more than five times.

3. Results

Ultrapure water was used as a sample. In Fig. 2, the number concentration distribution of nanobubble diameter in ultrapure water is shown for different irradiation time. Before ultrasonic irradiation, nanobubbles and nanoparticles are not detected in ultrapure water. Ultrasonic frequency was 22 kHz. The ultrasonic power was measured by calorimetry and adjusted to 15 W. After ultrasonic irradiation, nanobubbles of 50 – 220 nm in diameter are observed. This result means that ultrasonic irradiation to ultrapure water is able to generate bulk nanobubbles. The number concentration increases with irradiation time. By summing the number concentration distribution of nanobubble diameter, the number concentration of nanobubbles was calculated.

Fig. 3 shows the change in number concentration of nanobubbles in ultrapure water with

irradiation time for different ultrasonic power. The number concentration of nanobubbles increases with time. At the same irradiation time, the number concentration of nanobubbles becomes higher as ultrasonic power increases.

The effect of ultrasonic frequency on time change of number concentration of nanobubbles in ultrapure water is shown in Fig. 4. The ultrasonic power was 15 W. For all frequency, the number concentration of nanobubbles increases with time and seems to approach asymptotically to an equilibrium value. At the same irradiation time, the number concentration of nanobubbles increases with decreasing frequency.

Nanobubble water prepared by pressurized dissolution method was used as a sample. Before ultrasonic irradiation, the nanobubble diameter was in a range of 30 – 400 nm and the number concentration of nanobubbles was about 3.0×10^9 mL^{-1}.

The change in number concentration of nanobubbles in nanobubble water with irradiation time is shown for different ultrasonic frequency in Fig. 5. The ultrasonic power is 15 W. For all frequency, the number concentration of nanobubbles decreases with time and seems to approach asymptotically to an equilibrium value. At the same irradiation time, the number concentration of nanobubbles decreases with increasing frequency. The number concentration of nanobubbles decreased with increasing ultrasonic power.

4. Discussion

4.1 Modeling of number concentration of nanobubbles

It was found out that bulk nanobubbles were generated by ultrasonic irradiation to ultrapure water and reduced by irradiation to nanobubble water. The number concentration of nanobubbles approached asymptotically to an equilibrium value as ultrasonic irradiation time became longer. From these results, it is clear that generation and reduction of nanobubbles in water occur simultaneously by ultrasonic irradiation.

When ultrasound is irradiated to water, bubble nuclei grow to cavitation bubbles with expansion and compression, and finally collapse (Suslick, 1989). The cavitation bubble diameter just before collapse becomes to be about resonance bubble diameter (Leighton, 1994). In this experimental condition, the cavitation bubble diameter just before collapse is more than 1 μm because the resonance bubble diameter in water at 22 kHz and 1 MHz are estimated to be 150 μm and 6.6 μm from Minnaert equation, respectively (Minnaert, 1933; Devaud et al., 2008). Bubble nuclei are fine bubbles in liquid and gas pockets within crevices in solid particle and wall (Afel, 1984; Neppiras, 1984; Grieser et al., 2015). In this study, solid particles and fine bubbles, which were more than 30 nm in diameter, were not detected in ultrapure water by nanoparticle tracking analysis method. It is thought that bubble nuclei are nanobubbles less than 30 nm in diameter and gas pockets within crevices in vessel wall.

A simple model for generation and reduction of nanobubbles by ultrasonic irradiation is illustrated in Fig. 6. The bubble nuclei grow to cavitation bubbles with expansion and compression by way of nanobubbles. Cavitation bubbles mostly fragment into fine bubbles of various size such as bubble nuclei and nanobubbles due to collapse. The nanobubbles are generated due to the growth of bubble nuclei and the collapse of cavitation bubbles. The reduction in the concentration of nanobubbles is due to the growth of nanobubbles toward cavitation bubbles. Moreover, parts of nanobubbles and microbubbles aggregate by Bjerknes force and float to water surface.

We assume that generation and reduction of nanobubbles are independent of each other and simply express the changing rate of number concentration of nanobubbles as follows:

$$\frac{\mathrm{d}N}{\mathrm{d}t} = k_{\mathrm{g}} - k_{\mathrm{r}}N \tag{1}$$

where N is the number concentration of nanobubbles, k_{g} is the generation rate coefficient of nanobubbles, k_{r} is the reduction rate coefficient of nanobubbles, and t is ultrasonic irradiation time. Integration of Eq. (1) gives

$$N = \frac{k_g}{k_r} + C \exp(-k_r t) \quad (2)$$

where C is an integration constant. Before ultrasonic irradiation, the number concentration of nanobubbles is initial number concentration of nanobubbles N_0. The number concentration of nanobubbles is therefore

$$N = N_e + (N_0 - N_e)\exp(-k_r t) \quad (3)$$

where $N_e = k_g / k_r$ is an equilibrium number concentration of nanobubbles under ultrasonic irradiation. The calculated results obtained from Eq. (3) are also plotted in Figs. 3, 4, and 5 as curves and are in good agreement with the experimental data. This fact means that our model is able to explain behavior of generation and reduction of nanobubbles by ultrasonic irradiation.

Effects of ultrasonic frequency on the generation and the reduction rate coefficients of number concentration of nanobubbles are plotted in Figs. 7 (a) and (b). Samples are ultrapure and nanobubble water. In both water, the generation rate coefficient of nanobubbles becomes higher as the frequency decreases as shown in Fig. 7 (a). Tran *et al*. (2014) degraded polymer in solution by ultrasound and reported that mechanical effect of cavitation increased with decreasing frequency. Wang and Manmi (2014) numerically simulated microbubble dynamics under ultrasound. The maximum bubble radius just before collapse and the liquid jet velocity generated by the collapse of cavitation bubbles increased as the frequency became lower. Mason and Lorimer (1988) also reported that bubbles tended to be larger by a decrease of frequency and therefore their collapse was more violent. Form these facts, it is considered that violent collapse of cavitation bubbles at low frequency enhances the generation of nanobubbles. The generation rate coefficients for nanobubble water are higher than those for ultrapure water. In nanobubble water, it is thought that the generation of nanobubble due to the collapse of cavitation bubbles is enhanced since the number of cavitation bubbles increases by the growth of many nanobubbles.

In the case of ultrapure water, the reduction rate coefficient of nanobubbles slightly decreases with increasing frequency as shown in Fig. 7(b). In our previous paper, cavitation threshold, which is

minimum amplitude of sound pressure required to initiate cavitation, was investigated from 22 kHz to 4.88 MHz (Nguyen et. al., 2017). Cavitation threshold increased with increasing frequency. From these facts, it is thought that cavitation bubbles are hard to generate from nanobubbles at high frequency.

On the other hand, for the case of nanobubble water, the reduction rate coefficient at 22, 43, and 129 kHz are higher than those for ultrapure water and slightly decreases with frequency. However, at 488 kHz and 1 MHz, the reduction rate coefficients are much higher than those for ultrapure water and increases with frequency. Kobayashi et al. (2011) irradiated ultrasound at 2.4 MHz to water containing many microbubbles from the vessel bottom and observed that the rapid ascent of microbubbles was caused by their agglomeration. They explained that agglomeration of microbubbles was occurred by primary and secondary Bjerknes force (Leighton, 1994). Lee et al. (2011) reported that when ultrasound at 448 and 726 kHz was irradiated to water, generated visible bubbles were driven toward the liquid surface. However, visible bubbles were trapped in standing wave at 168 kHz. They explained that a radiation force by traveling wave moved bubbles because the increase in the attenuation of ultrasound reduced the amplitude of reflective wave at high frequency.

The radiation force acting on one nanobubble is negligible small because of its small volume. However, when frequency and nanobubble concentration are high, it is thought that larger nanobubbles due to agglomeration or coalescence are formed because secondary Bjerknes force becomes large. The secondary Bjerknes force is proportional to the squares of frequency and inversely proportional to the squares of distance between bubbles (Leighton, 1994). As the radiation force acts on larger nanobubbles, a part of nanobubbles may flow upward and disappear at liquid surface. From these reasons, the reduction rate coefficient in nanobubble water significantly increases at 488 kHz and 1 MHz.

The effect of ultrasonic frequency on the equilibrium number concentration of nanobubbles in ultrapure and nanobubble water is plotted in Fig. 8. The equilibrium number concentrations of nanobubbles in ultrapure water are same as those in nanobubble water. As shown in Eq. (3), the

equilibrium number concentration is expressed as the ratio of the generation rate coefficient to the reduction rate coefficient. The equilibrium number concentration was independent of ultrasonic power. The equilibrium number concentration increases with decreasing ultrasonic frequency. This is because the generation of nanobubbles is enhanced at low frequency. The equilibrium number concentration in nanobubble water are equal to those in ultrapure water. This means that the equilibrium number concentration is independent of initial number concentration of nanobubble. During ultrasonic irradiation to ultrapure water, the number concentration of nanobubbles is always lower than the equilibrium number concentration. On the other hand, during irradiation to high concentration nanobubble water, the number concentration is always higher than the equilibrium number concentration. The generation and reduction rate constants depend on whether initial number concentration is lower or higher than the equilibrium number concentration but do not depend on value of initial number concentration.

4.2 Mode diameter of nanobubbles

Fig. 9 shows the effect of ultrasonic frequency on the mode diameter of nanobubbles at 5 and 30 minutes irradiation in ultrapure water. The mode diameter of nanobubbles generated by ultrasound are within 90 - 100 nm. Effects of frequency and irradiation time on the mode diameter are small. From this result, it is found that the nanobubbles of 90 - 100 nm are easily to generate by ultrasound.

In Fig. 10, the change in mode diameter of nanobubbles in nanobubble water with irradiation time is shown for different ultrasonic frequency at 15 W. Before ultrasonic irradiation, the mode diameter is about 120 nm. In the cases at 22, 43, and 129 kHz, the mode diameter decreases to 80 - 90 nm. Dissolved oxygen of nanobubble water after irradiation was lower than initial value and became smaller as the frequency became higher. From these results, it thought that a part of nanobubbles of 120 nm in diameter dissolves by ultrasonic stimulation and reduces the diameter to 80 - 90 nm though most of nanobubbles grow to cavitation bubbles. Tuziuti et al. (2018) reported that

nanobubble concentration decreased by addition of degassed water due to dissolution. Except for 22 kHz, the mode diameters have minimum values. The irradiation time at minimum diameter becomes shorter as the ultrasonic frequency increases. This may be because the number of times of ultrasonic stimulation spatially and temporally increases and the dissolution of nanobubbles accelerates in water of low dissolved oxygen. On the other hand, the cases at 488 kHz and 1 MHz, the mode diameter initially decreases to minimum value and increases after dissolved oxygen in nanobubble water became constant. This increment might be because nanobubble aggregations coalesce due to secondary Bjerknes force as discussed in Fig. 7(b). Moreover, large bubbles may grow at the expense of smaller bubbles due to Ostwald ripening (Chang et al. 2008; Watanabe et al. 2014). Change in number concentration and mode diameter of nanobubbles with standing time and effects of dissolved oxygen should be investigated within near future.

5. Conclusions

In this study, ultrasound was irradiated to ultrapure water and high concertation nanobubble water. In the case of ultrapure water, bulk nanobubbles were generated and mode diameter of nanobubbles was 90 – 100 nm. Number density of nanobubbles increased with increasing ultrasonic power and decreasing frequency. On the other hand, for the case of high concertation nanobubble water, bulk nanobubbles reduced by ultrasound. Number concentration of nanobubbles decreased with increasing ultrasonic power and frequency. In both water, the number concentration of nanobubbles exponentially changed with time and approached asymptotically to an equilibrium value.

We assumed that generation and reduction of nanobubbles in water occurred simultaneously by ultrasound and are independent of each other. The changing rate of number concentration of nanobubbles was simply modeled. The generation rate coefficient of number concentration of nanobubbles decreased as ultrasonic frequency increased. In the case of ultrapure water, the reduction rate coefficient of nanobubbles slightly decreased with increasing frequency. However, for the case

of nanobubble water, the reduction rate constant at 488 kHz and 1 MHz became much higher than those in ultrapure water. The equilibrium number concentration of nanobubbles in ultrapure water were equal to those in nanobubble water and decreased with increasing frequency. The results calculated by our model were in good agreement with the experimental data. Our model was able to explain behavior of generation and reduction of nanobubbles by ultrasonic irradiation.

From this study, it is found that bulk nanobubbles are generated by ultrasonic irradiation to water. The nanobubble generator using ultrasound is compact, simple in operation and has a short generation time. This method is contamination-free because the liquid pump is unnecessary. Moreover, it is able to control the number concentration of nanobubbles by selecting ultrasonic frequency and power.

Acknowledgements

This work was supported by Grant-in-Aid for Scientific Research (B) Number 16H04560 from Japan Society for the Promotion of Science.

Reference

Apfel, R.E., 1984. Acoustic cavitation series: part four acoustic cavitation inception, Ultrasonics 22(4), 167-173.

Agarwal, A., Ng, W.J., Liu, Y., 2011. Principle and applications of microbubble and nanobubble technology for water treatment, Chemosphere 84(9), 1175-1180. https://doi.org/10.1016/j.chemosphere.2011.05.054.

Alheshibri, M., Qian, J., Jehannin, M., Craig, V.J., 2016. A history of nanobubbles, Langmuir 32(43), 11086-11100. https://doi.org/10.1021/acs.langmuir.6b02489.

Cai, W.B., Yang, H.L., Zhang, J., Yin, J.K., Yang, Y.L., Yuan, L.J., Zhang, L., Duan, Y.Y., 2015. The optimized fabrication of nanobubbles as ultrasound contrast agents for tumor imaging, Sci. Rep. 5, 13725. https://doi.org/10.1038/srep13725.

Chang, F.-M., Sheng, Y.-J., Cheng, S.-L., Tsao, H.-K., 2008. Tiny bubble removal by gas flow through porous superhydrophobic surfaces: Ostwald ripening, Appl. Phys. Lett. 92(26), 264102. https://doi.org/10.1063/1.2953703.

Cosgrove, D., 2006. Ultrasound contrast agents: an overview, Eur. J. Radiol. 60(3), 324-330. https://doi.org/10.1016/j.ejrad.2006.06.022.

Devaud, M., Hocquet, T., Bacri, J.-C., Leroy, V., 2008. The Minnaert bubble: an acoustic approach, Eur. J. Phys. 29(6), 1263-1285. https://doi.org/10.1088/0143-0807/29/6/014.

Ebina, K., Shi, K., Hirao, M., Hashimoto, J., Kawato, Y., Kaneshiro, S., Morimoto, T., Koizumi, K., Yoshikawa, H., 2013. Oxygen and air nanobubble water solution promote the growth of plants, fishes, and mice, Plos One 8(6), e65339. https://doi.org/10.1371/journal.pone.0065339.

Grieser, F., Choi, P.-K., Enomoto, N., Harada, H., Okitsu, K., Yasui, K., 2015. Sonochemistry and the Acoustic Bubbles, Elsevier.

Jing, H., Cheng, W., Li, S., Wu, B., Leng, X., Xu, S., Tian, J., 2016. Novel cell-penetrating peptide-loaded nanobubbles synergized with ultrasound irradiation enhance EGFR siRNA delivery for

triple negative Breast cancer therapy, Colloid. Surfaces B 146(1), 387-395. https://doi.org/10.1016/j.colsurfb.2016.06.037.

Kobayashi, D., Hayashida, Y., Sano, K., Terasaka, K., 2011. Agglomeration and rapid ascent of microbubbles by ultrasonic irradiation, Ultrason. Sonochem. 18(5), 1193-1196. https://doi.org/10.1016/j.ultsonch.2010.11.005.

Kukizaki, M., Goto, M., 2006. Size control of nanobubbles generated from Shirasu-porous-glass (SPG) membranes, J. Membrane Sci. 281(1-2), 386-396. https://doi.org/10.1016/j.memsci.2006.04.007.

Lee, J., Ashokkumar, M., Yasui, K., Tuziuti, T., Kozuka, T., Towata, A., Iida, Y., 2011. Development and optimization of acoustic bubble structures at high frequencies, Ultrason. Sonochem., 18(1), 92-98. https://doi.org/10.1016/j.ultsonch.2010.03.004.

Leighton, T.G., 1994. The Acoustic Bubble, Academic Press.

Liu, S., Kawagoe, Y., Makino, Y., Oshita, S., 2013. Effects of nanobubbles on the physicochemical properties of water: the basis for peculiar properties of water containing nanobubbles, Chem. Eng. Sci. 93, 250-256. https://doi.org/10.1016/j.ces.2013.02.004.

Liu, S., Oshita, S., Kawabata, S., Makino, Y., Yoshimoto, T., 2016. Identification of ROS produced by nanobubbles and their positive and negative effects on vegetable seed germination, Langumir 32(43), 11295-11302. https://doi.org/10.1021/acs.langmuir.6b01621.

Luján-Facundo, M.J., Mendoza-Roca, J.A., Cuartas-Uribe, B., Álvarez-Blanco, S., 2016. Cleaning efficiency enhancement by ultrasounds for membranes used in dairy industries, Ultrason. Sonochem. 33, 18-25. https://doi.org/10.1016/j.ultsonch.2016.04.018.

Maeda, S., Kobayashi, H., Ida, K., Kashiwa, M., Nishihara, I., Fujita, T., 2014. The effect of dilution on the quantitative measurement of bubbles in high-density ultrafine bubble-filled water using the light scattering method, Proc. SPIE 9232, 92320V. https://doi.org/10.1117/12.2064810.

Mason, T.J., Lorimer, J.P., Theory, Applications and Uses of Ultrasound in Chemistry, 1988. Ellis Harwood Limited

Matsuno, H., Ohta, T., Shundo, A., Fukunaga, Y., Tanaka, K., 2014. Simple surface treatment of cell-culture scaffolds with ultrafine bubble water, Langumir 30(50), 15238-15243. https://doi.org/10.1021/la5035883.

Miastkowska, M.A., Banach, M., Pulit-Prociak, J., Sikora, E.S., Głogowska, A., Zielina, M., 2017. Statistical analysis of optimal ultrasound emulsification parameters in thistle-oil nanoemulsions, J. Surfact. Deterg. 20(1), 233-246. https://doi.org/10.1007/s11743-016-1887-7.

Minamikawa, K., Takahashi, M., Makino, T., Tago, K., Hayatsu, M., 2015. Irrigation with oxygen-nanobubble water can reduce methane emission and arsenic dissolution in a flooded rice paddy Environ. Res. Lett. 10(8), 084012. https://doi.org/10.1088/1748-9326/10/8/084012.

Minnart, M., 1933. Air bubble and sound of running water, Phil. Mag. 6, 235-248.

Mogami, K., Aoki, K., Yonezawa, Y., Hiraki, K., Tanaka, H., 2013. Japanese patent, 2013-086161 (in Japanese)

Neppiras, E.A., 1984. Acoustic cavitation series: part one acoustic cavitation: an introduction, Ultrasonics 22(1), 25-28.

Nguyen, T.T., Asakura, Y., Koda, S., Yasuda, K., 2017. Dependence of cavitation, chemical effect, and mechanical effect thresholds on ultrasonic frequency, Ultrason. Sonochem. 39, 301-306. https://doi.org/10.1016/j.ultsonch.2017.04.037.

Noguchi, T., Ebina, K., Hirao, M., Morimoto, T., Koizumi, K., Kitaguchi, K., Matsuoka, H., Iwahashi, T., Yoshikawa, H., 2017. Oxygen ultra-fine bubbles water administration prevents bone loss of glucocorticoid-induced osteoporosis in mice by suppressing osteoclast differentiation, Osteoporos Int. 28(3), 1063-1075. https://doi.org/10.1007/s00198-016-3830-1.

Oh, S.H.. Yoon, S.H., Song, H., Han, J.G., Kim, J.-M., 2013. Effect of hydrogen nanobubble addition on combustion characteristics of gasoline engine, Int. J. Hydrogen Energ. 38(34), 14849-14853. https://doi.org/10.1016/j.ijhydene.2013.09.063.

Oh, S.H., Kim, J.-M., 2017, Generation and stability of bulk nanobubbles, Langumir 33(15), 3818-3823. https://doi.org/10.1021/acs.langmuir.7b00510.

Safonov, V.L., Khitrin, A.K., 2013. Hydrogen nanobubbles in a water solution of dietary supplement, Colloids Surfaces A 436, 333-336. https://doi.org/10.1016/j.colsurfa.2013.06.043.

Schenk, H.J., Steppe, K., Jansen, S., 2015. Nanobubbles: a new paradigm for air-seeding in xylem, Trends Plant Sci. 20(4), 199-205. https://doi.org//10.1016/j.tplants.2015.01.008.

Suslick, K.S., 1989, The chemical effects of ultrasound, Sci. Am. 260(2), 80-87.

Suzuki, R., Oda, Y., Omata, D., Nishiie, N., Koshima, R., Shiono, Y., Sawaguchi, Y., Unga, J., Naoi, T., Negishi, Y., Kawakami, S., Hashida, M., Maruyama, K., 2016. Tumor growth suppression by the combination of nanobubbles and ultrasound, Cancer Sci. 107(3), 217-223. https://doi.org/10.1111/cas.12867.

Temesgen, T., Bui, T.T., Han, M., Kim, T., Park, H., 2017. Micro and nanobubble technologies as a new horizon for water-treatment techniques: a review, Adv. Colloid Interf. Sci. 246, 40-51. https://doi.org/10.1016/j.cis.2017.06.011.

Tran, K.V.B., Kimura, T., Kondo, T., Koda, S., 2014. Quantification of frequency dependence of mechanical effects induced by ultrasound, Ultrason. Sonochem. 21(2), 716-721. https://doi.org/10.1016/j.ultsonch.2013.08.018.

Tsuji, H., 2013, United states patent, No.8523151 B2

Tuziuti, T., Yasui, K., Kanematsu, W., 2018. Influence of addition of degassed water on bulk nanobubbles, Ultrason. Sonochem. 43, 272-274. https://doi.org/10.1016/j.ultsonch.2018.01.015.

Ushida, A., Hasegawa, T., Takahashi, N., Nakajima, T., Murao, S., Narumi, T., Uchiyama, H., 2012. Effect of mixed nanobubble and microbubble liquids on the washing rate of cloth in an alternating flow, J. Surfact. Deterg. 15(6), 695-702. https://doi.org/10.1007/s11743-012-1348-x.

VanOsdol, J., Ektate, K., Ramasamy, S., Maples, D., Collins, W., Malayer, J., Ranjan, A., 2017. Sequential HIFU heating and nanobubble encapsulation provide efficient drug penetration from stealth and temperature sensitive liposomes in colon cancer, J. Controll. Release 247, 55-63. https://doi.org/10.1016/j.jconrel.2016.12.033.

Wang, Q.X., Manmi, K., 2014. Three dimensional microbubble dynamics near a wall subject to high

intensity ultrasound, Phys. Fluids 26(3), 032104. https://doi.org/10.1063/1.4866772.

Wang, J.-P., Zhou, X.-L., Yan, J.-P., Zheng, R.-Q., Wang, W., 2017. Nanobubbles as ultrasound contrast agent for facilitating small cell lung cancer imaging, Oncotarget 8(44), 78153-78162. https://doi.org/10.18632/oncotarget.18155.

Watanabe, H., Suzuki, M., Inaoka, H., Ito, N., 2014, Ostwald ripening in multiple-bubble nuclei, J. Phys. Chem. 141(23), 234703. https://doi.org/10.1063/1.4903811.

Wu, Z., Chen, H., Dong, Y., Mao, H., Sun, J., Chen, S., Craig, V.S.J., Hu, J., 2008. Cleaning using nanobubbles: defouling by electrochemical generation of bubbles, J. Colloid Interf. Sci. 328(1), 10-14. https://doi.org/10.1016/j.jcis.2008.08.064.

Yasui, K., Tuziuti, T., Kanematsu, W., Kato, K., 2016. Dynamic equilibrium model for a bulk nanobubble and a microbubble partly covered with hydrophobic material, Langmuir 32(43), 11101-1110. https://doi.org/10.1021/acs.langmuir.5b04703.

Yang, H., Deng, L., Li, T., Shen, X., Yan, J., Zuo, L., Wu, C., Liu, Y., 2015. Multifunctional PLGA nanobubbles as theranostic agents: combining doxorubicin and P-gp siRNA co-delivery into human breast cancer cells and ultrasound cellular imaging, J. Biomed. Nanotechnol. 11(12), 2124-2136. https://doi.org/10.1166/jbn.2015.2168.

Zhu, J., An, H., Alheshibri, M., Liu, L., Terpstra, P.M.J., Liu, G., Craig, V.S.J., 2016. Cleaning with bulk nanobubbles, Langumir 32(43), 11203-11211. https://doi.org/10.1021/acs.langmuir.6b01004.

Figure captions

Fig. 1. Outline of experimental apparatus.

Fig. 2. Number concentration distribution of nanobubble diameter in ultrapure water for different irradiation time at 22 kHz and 15 W.

Fig. 3. Change in number concentration of nanobubbles in ultrapure water with irradiation time for different ultrasonic power at 22 kHz.

Fig. 4. Effect of ultrasonic frequency on time change of number concentration of nanobubbles in ultrapure water at 15 W.

Fig. 5. Change in number concentration of nanobubbles in nanobubble water with irradiation time for different ultrasonic frequency at 15 W.

Fig. 6. Model for generation and reduction of nanobubbles by ultrasonic irradiation.

Fig. 7. Effects of ultrasonic frequency on the generation (a) and the reduction (b) rate coefficients of number concentration of nanobubbles in ultrapure and nanobubble water.

Fig. 8. Effect of ultrasonic frequency on the equilibrium number concentration of nanobubbles in ultrapure and nanobubble water.

Fig. 9. Effect of ultrasonic frequency on the mode diameter of nanobubbles at 5 and 30 minutes irradiation in ultrapure water.

Fig. 10. Change in mode diameter of nanobubbles in nanobubble water with irradiation time for different ultrasonic frequency at 15 W.

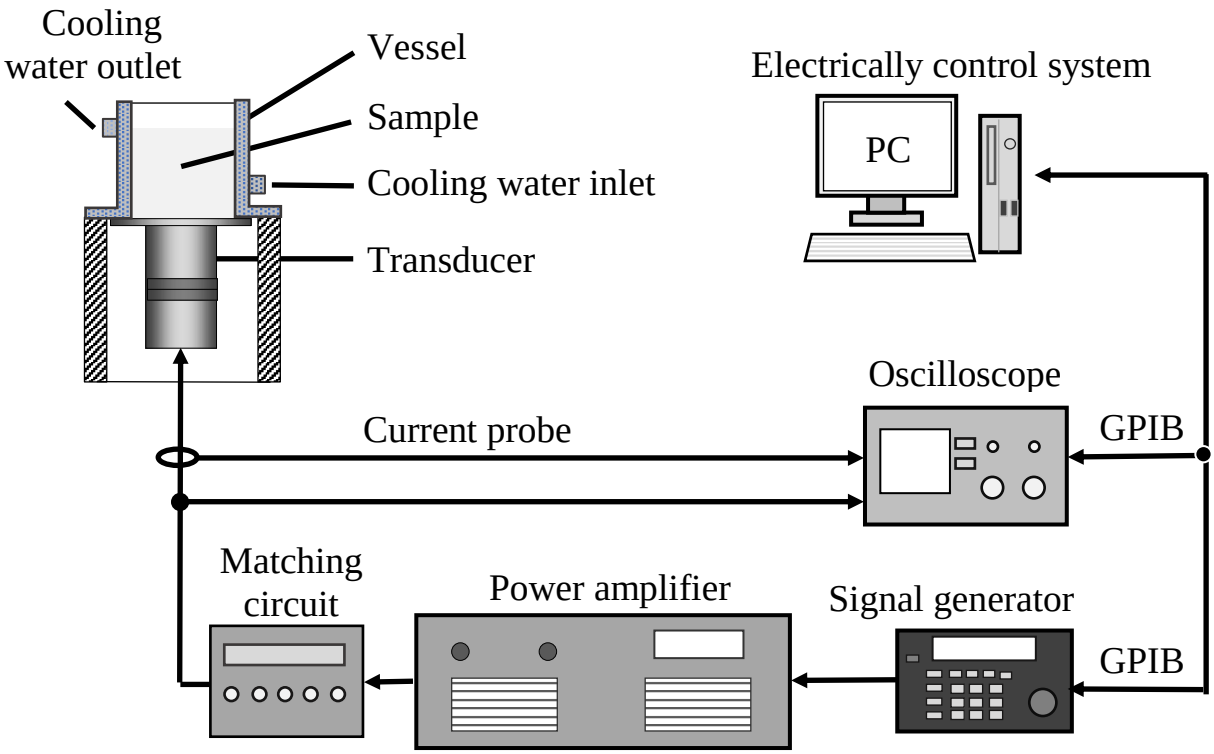

Fig. 1. Outline of experimental apparatus.

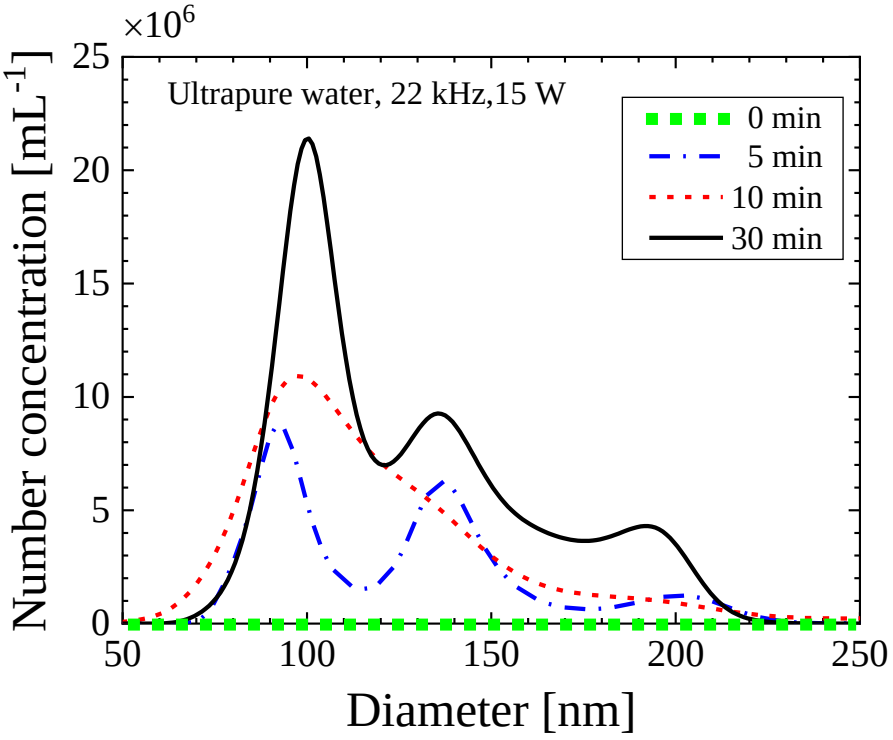

Fig. 2. Number concentration distribution of nanobubble diameter in ultrapure water for different irradiation time at 22 kHz and 15 W.

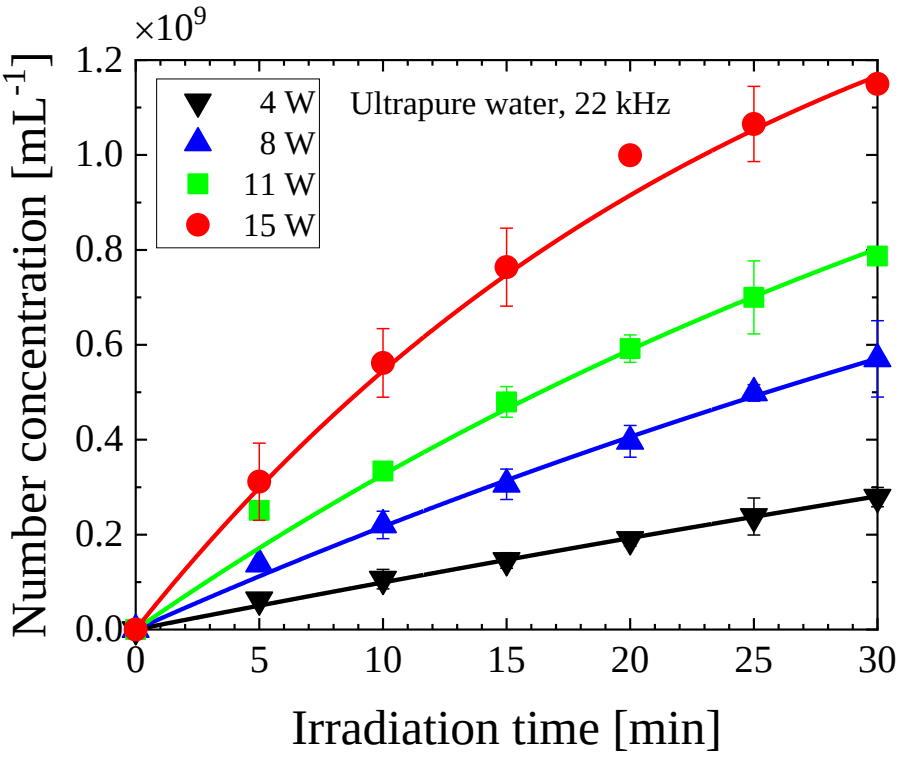

Fig. 3. Change in number concentration of nanobubbles in ultrapure water with irradiation time for different ultrasonic power at 22 kHz.

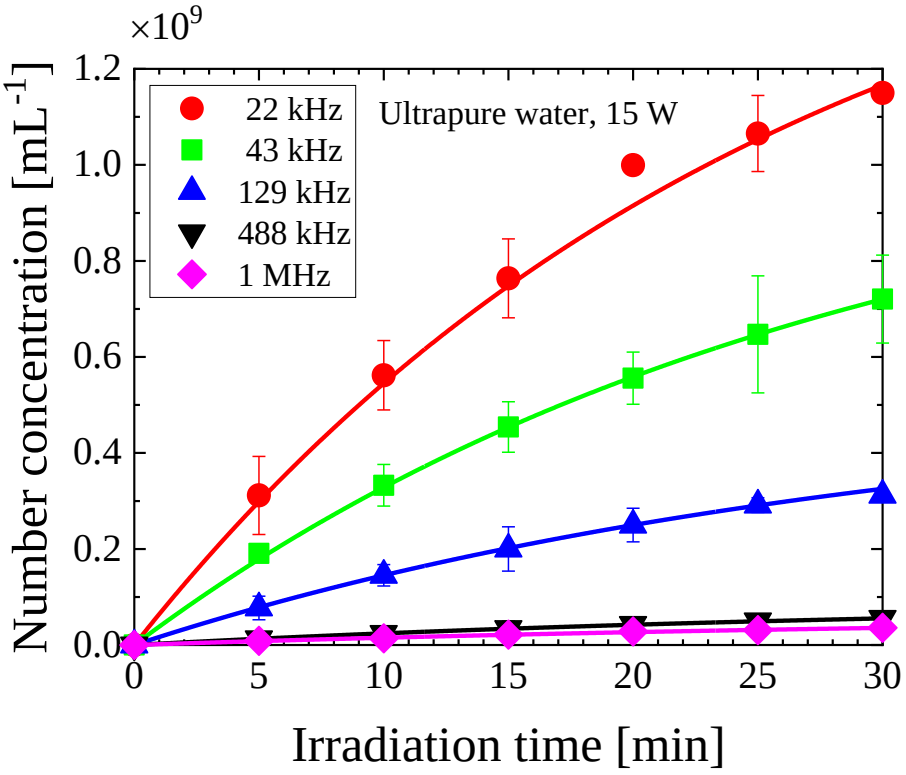

Fig. 4. Effect of ultrasonic frequency on time change of number concentration of nanobubbles in ultrapure water at 15 W.

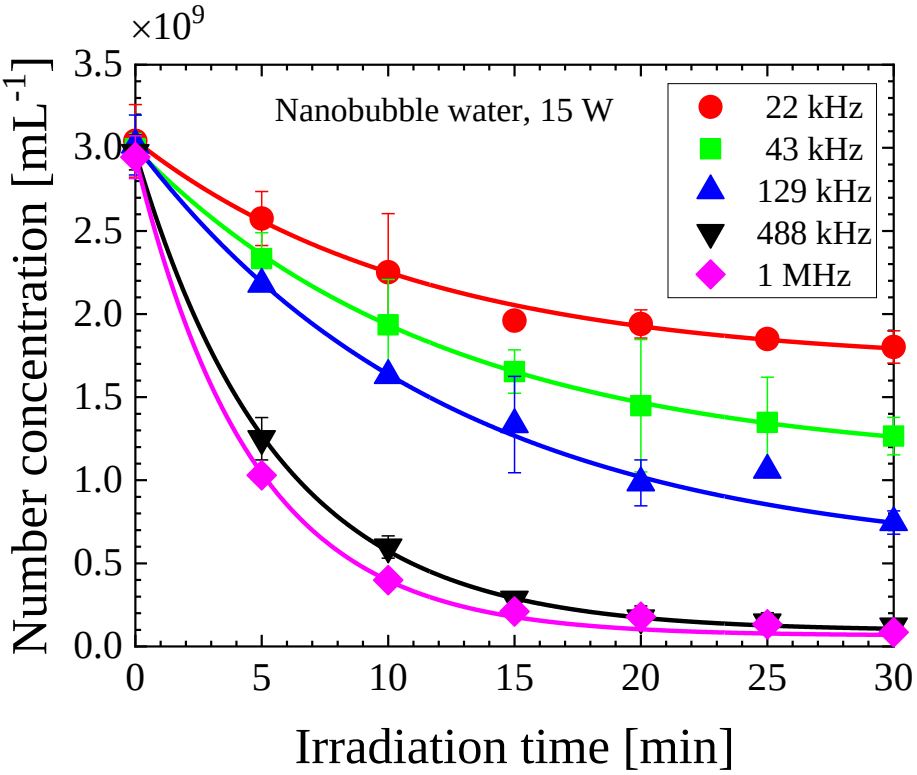

Fig. 5. Change in number concentration of nanobubbles in nanobubble water with irradiation time for different ultrasonic frequency at 15 W.

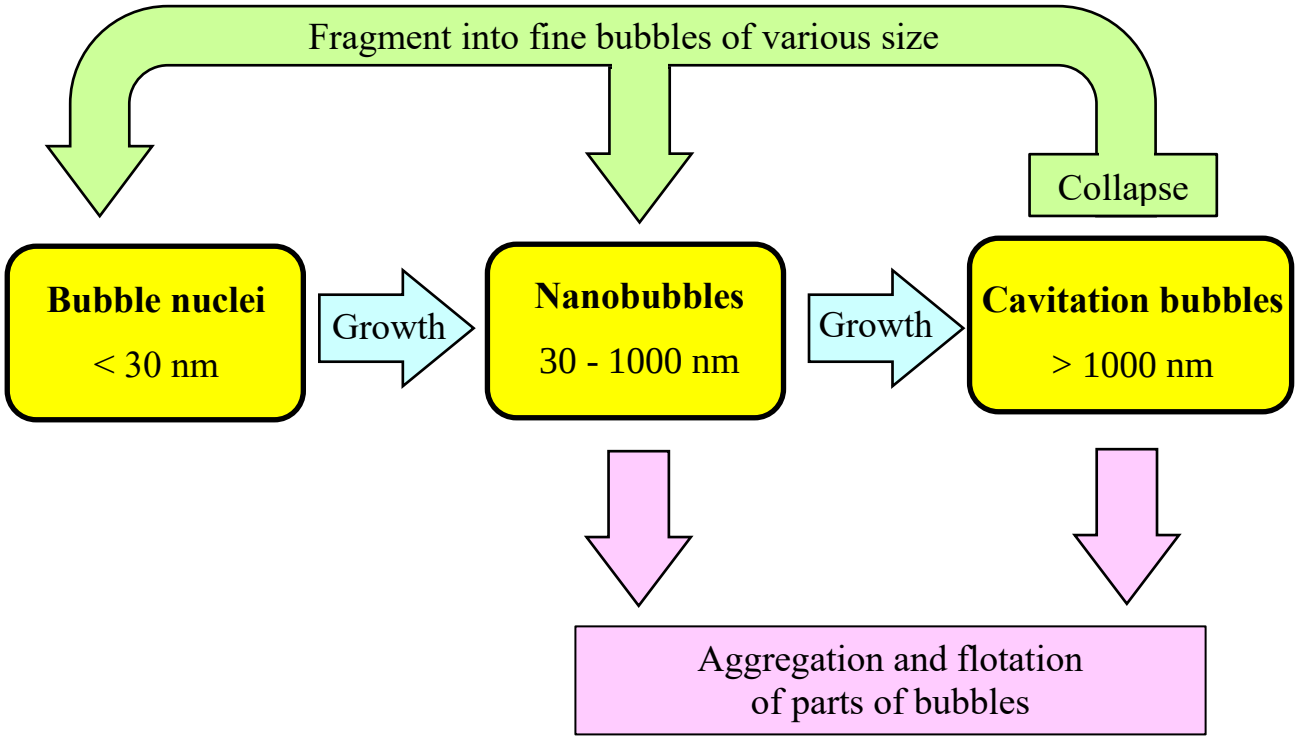

Fig. 6. Model for generation and reduction of nanobubbles by ultrasonic irradiation.

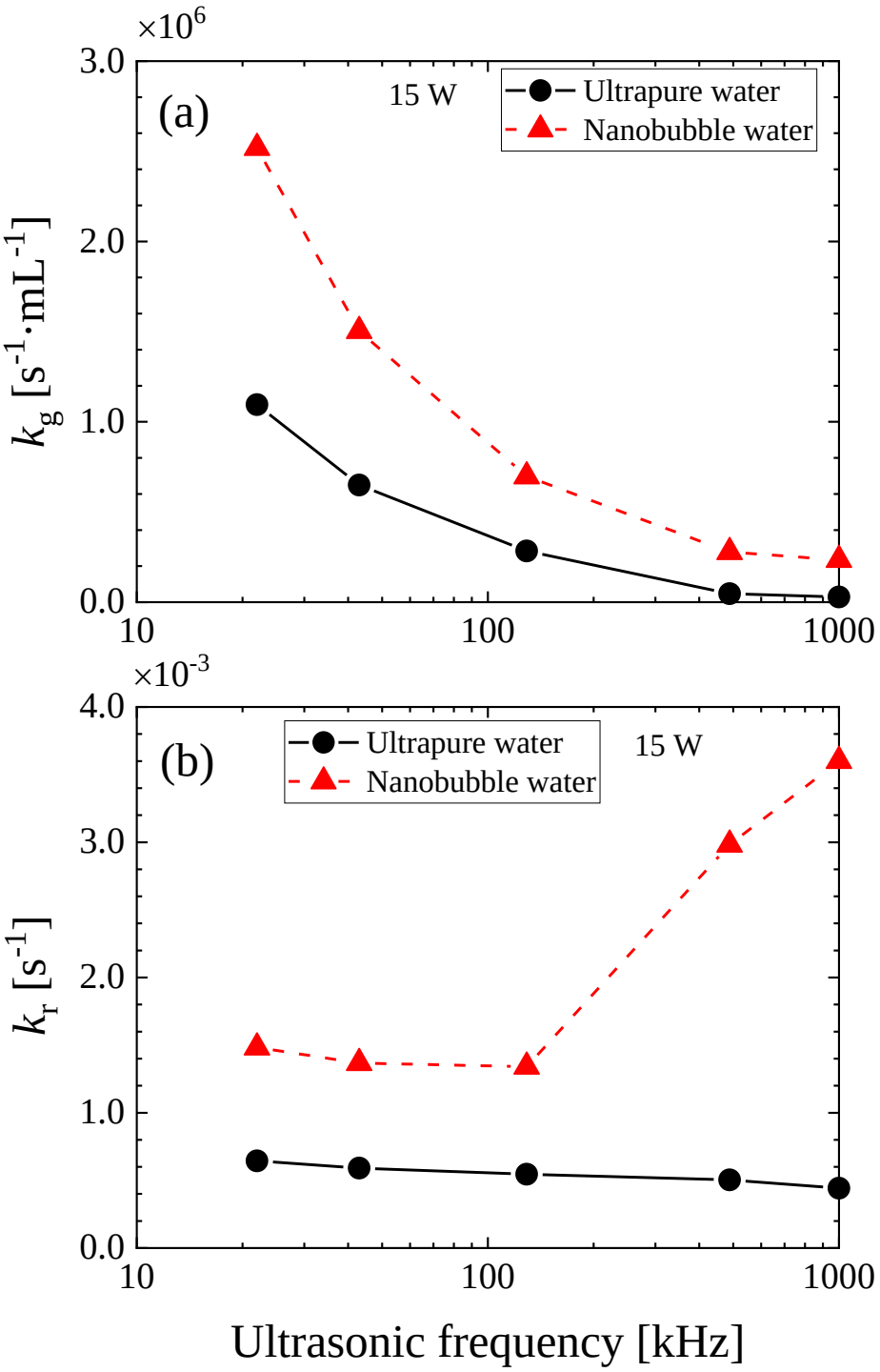

Fig. 7. Effects of ultrasonic frequency on the generation (a) and the reduction (b) rate coefficients of number concentration of nanobubbles in ultrapure and nanobubble water.

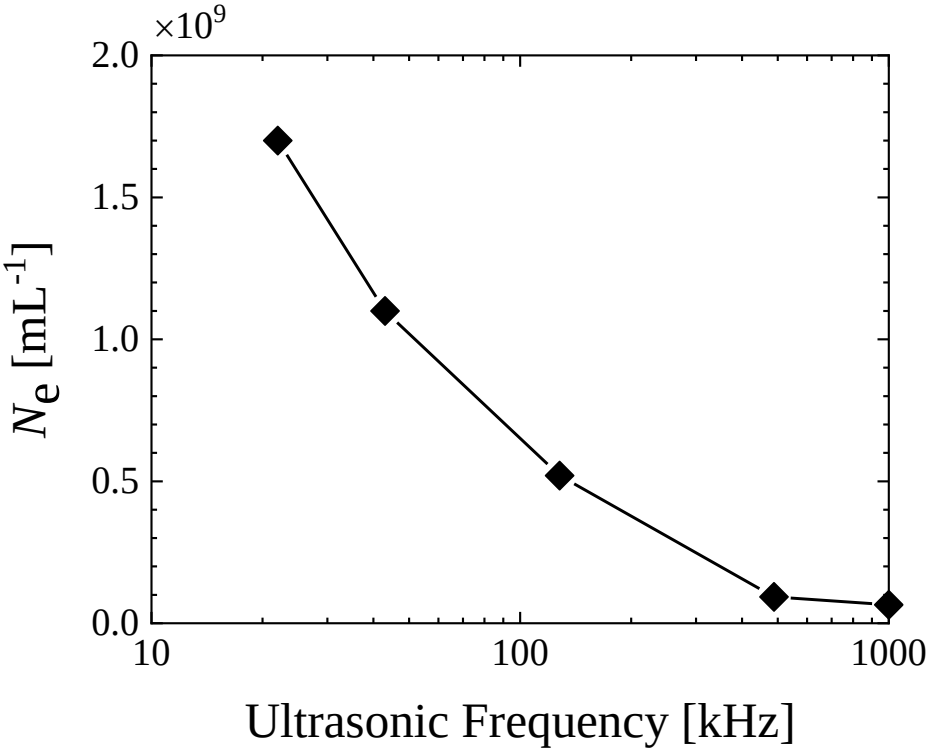

Fig. 8. Effect of ultrasonic frequency on the equilibrium number concentration of nanobubbles in ultrapure and nanobubble water.

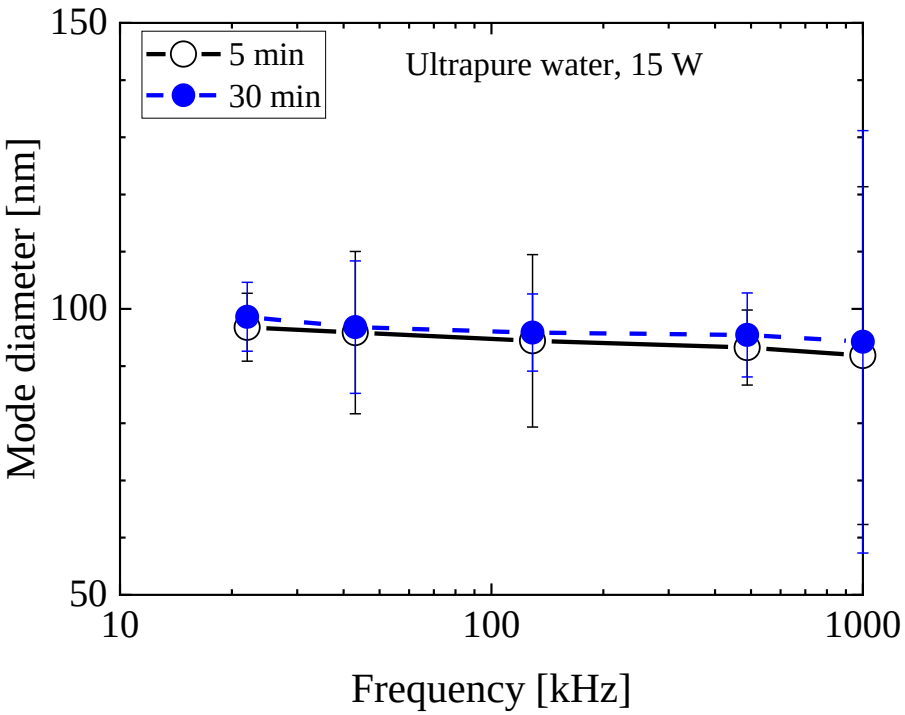

Fig. 9. Effect of ultrasonic frequency on the mode of nanobubbles at 5 and 30 minutes irradiation in ultrapure water.

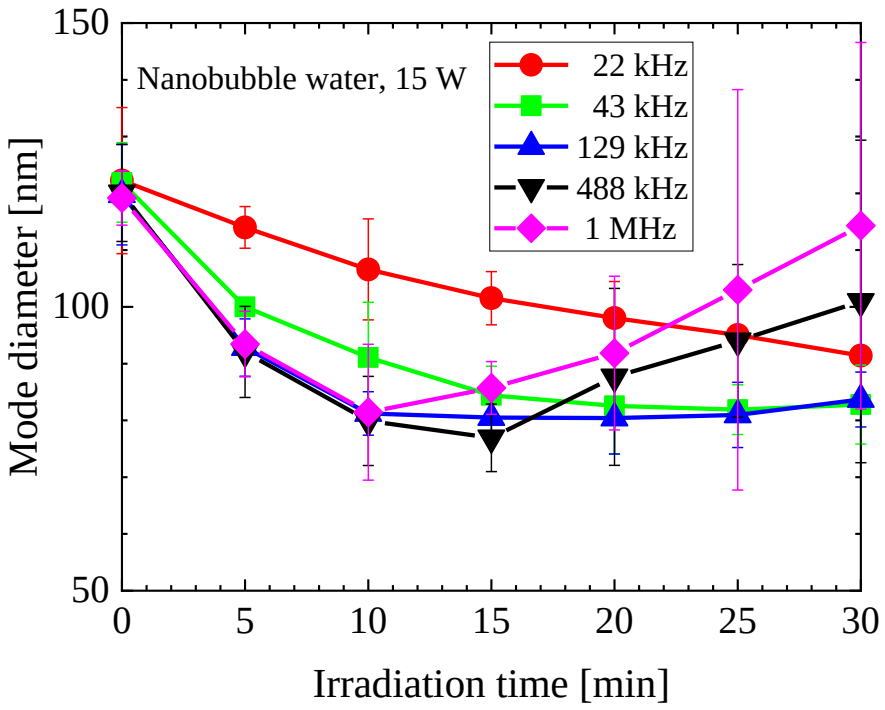

Fig. 10. Change in mode diameter of nanobubbles in nanobubble water with irradiation time for different ultrasonic frequency at 15 W.